A R C H I V E S O F M E T A L L U R G Y A N D M A T E R I A L S
Volume 55 2010 Issue 3

K. JANERKA*, D. BARTOCHA*, J. SZAJNAR*, J. JEZIERSKI*

THE CARBURIZER INFLUENCE ON THE CRYSTALLIZATION PROCESS AND THE MICROSTRUCTURE OF SYNTHETIC CAST IRON

WPŁYW RODZAJU MATERIAŁU NAWĘGLAJĄCEGO NA PROCES KRZEPNIĘCIA I STRUKTURĘ ŻELIWA SYNTETYCZNEGO

The problems of synthetic cast iron production on the steel scrap and various carburizers (natural and synthetic graphite, petroleum coke, anthracite, cupola coke and charcoal) basis were presented in the paper. Until now the authors in their papers had analyzed mainly carbon assimilation by the liquid metal rate (recarburization efficiency) when these carburizers and various methods of recarburization were used [1,2,3,4]. The analysis covered the chemical composition and the properties of carburizers commonly used in foundries [5,6] and mechanical properties of the cast iron obtained on the steel scrap basis, too [2,7,8,9]. The computer modeling of heating and dissolution of carburizers' particles inside liquid metal were carried out, too [10,11].

The crystallization process of the synthetic cast iron analysis and that produced on pig iron basis for comparison were presented. There was observed that the carburizers change the DTA (Derivative Thermal Analysis) curves in specific temperature ranges. The authors presented some experimental results in form of recorded DTA curves. The presented results show also carburizers microstructures and synthetic cast iron and made on pig iron basis structures, too. The problems given under consideration in the paper has a purpose of set up a discussion on "heredity of cast iron" – some charging materials properties transferred to cast iron. Does such an issue exist and if yes, in what extent it decides of melted alloys properties (synthetic cast iron in described example)?

Keywords: synthetic cast iron, cast iron recarburization, cast iron microstructure, carburizer, solidification and crystallization

W artykule przedstawiono zagadnienia związane z wytwarzaniem żeliwa syntetycznego na bazie złomu stalowego i różnych rodzajów materiałów nawęglających (grafitu naturalnego i syntetycznego, koksu naftowego, antracytu, koksu odlewniczego i węgla drzewnego). Dotychczas autorzy w swoich publikacjach analizowali przede wszystkim stopień przyswojenia węgla przez ciekły metal (efektywność nawęglania) przy stosowaniu tych nawęglaczy i różnych metod nawęglania [1,2,3,4]. Analiza obejmowała również skład chemiczny i własności najczęściej stosowanych w odlewnictwie nawęglaczy [5,6] oraz własności mechaniczne żeliwa wytopionego na bazie złomu stalowego [2,7,8,9]. Prowadzone są również symulacje komputerowe procesu nagrzewania i rozpuszczania cząstek nawęglaczy znajdujących się w ciekłym metalu [10,11].

W artykule przedstawiono analizę procesu krzepnięcia żeliwa syntetycznego i dla porównania żeliwa uzyskanego na bazie surówki. Zauważono, że materiały nawęglające zmieniają przebieg krzywych Analizy Termiczno Derywacyjnej w pewnych zakresach temperatury. Autorzy przedstawili część uzyskanych wyników pomiarów w postaci zarejestrowanych krzywych ATD. Zaprezentowany materiał obejmuje również struktury materiałów nawęglających i struktury żeliwa syntetycznego oraz wytopionego na bazie surówki. Podjęta w artykule tematyka ma na celu wywołanie dyskusji o "dziedziczności" cech materiałów wsadowych przenoszonych do żeliwa. Czy takie zagadnienie istnieje i w jakim stopniu decyduje o własnościach wytopionych materiałów (w analizowanym przypadku żeliwa syntetycznego)?

1. Introduction

Cast iron is the most common casting alloy. In 2006 the part of castings made of grey cast iron, alloy cast iron and ductile cast iron in the total castings production was 65% (50% grey and alloy iron, 15% ductile iron) [12]. The wide use of this material is caused by good casting and technological properties and simple melting technique. The cast iron manufacturing process can be carried out with use of various charging materials. It can be based on pig iron with the returns and steel scrap additions. Nowadays more and more foundries limit or eliminate the pig iron from charge and replace it with steel scrap. Such approach results in production costs decrease but the recarburization process

* DEPARTMENT OF FOUNDRY, FACULTY OF MECHANICAL ENGINEERING, SILESIAN UNIVERSITY OF TECHNOLOGY, 44-100 GLIWICE, 7 TOWAROWA, POLAND

becomes necessary. The most important carburizers for cast iron recarburization in foundries are: natural and synthetic graphite, petroleum coke and anthracite. The natural graphite is a carbon material which contains generally a lot of mineral impurities such a crystalline schist, quartz, silicates, magnesium, aluminum and mica. The chemical composition of the natural graphite changes inside wide range depends on these impurities content. The synthetic graphite is obtained during petroleum coke or anthracite graphitization process at the temperature 2500-3000 Celsius degrees. The commonly used are Acheson's and Castner's methods [13]. The petroleum coke is a solid carbon product of oil distillation residues thermal treatment. It is susceptible to graphitization and may achieve high degree of crystalline structure order during the process. The anthracite is a natural carbon material with particularly high content of elemental carbon and low volatile parts and mineral impurities level. The minerals concentration and chemical composition of the anthracite depends on its origin [13].

Typical carburizers' chemical composition used during the experiments were shown in Table 1. Carbon content (C) in samples varies from 85% for the natural graphite to 99.35% for the synthetic graphite.

TABLE 1
Chemical composition of the carburizers [2]

Chemical composition	C %	S %	Volatile parts %	Ash %	Moisture content %
Natural graphite GN	85.00	0.08	3.00	11.00	2.00
Anthracite A	94.60	0.10	0.88	4.47	0.10
Synthetic graphite GS	99.35	0.015	0.08	0.57	0.09
Petroleum coke KN	99.25	0.82	0.27	0.48	0.10

Good carburizer should have high carbon content (>95%), low sulfur content (<0.3%), volatile parts (<1%) and should not contain more than 0.9% of moisture [7,14]. The impurities in the carburizer decrease carbon assimilation rate, increase slag volume and cause deterioration of produced alloys quality. The process rate and mass transfer coefficient are decreased, too. Due to higher carbon dissolution rate in cast iron, the use of the synthetic graphite is better, but its much higher cost causes the necessity of cheaper anthracite and petroleum coke based carburizers use.

2. The properties and morphology of the carburizers

From the crystalline structure order point of view two groups can be distinguished among the carbonaceous materials. The first group, which are polycrystalline graphite materials, the main structural components are graphite crystallites. The second group are less ordered carbonaceous materials and their main structural components are built of graphen layers packets, approximately parallel but randomly ordered along perpendicular to their surface direction and such appearance is so-called turbostratic crystallite [6,15,16,17].

The X-ray analysis of the carburizers shown in table 1 was carried out with use of X-ray diffractometer Xpert with cobalt lamp (Co $K_{\alpha 1}$; λ = 1.78901Å). The measurements were taken in ambient temperature inside the angle range 2θ from 10 to 100° (resolution 0.03°) [6].

X-ray patterns for less ordered carbonaceous materials (anthracite, petroleum coke) contain less visible fundamental reflections so they are difficult to interpretation. The degree of structure order can be worked out only by comparison with diffraction patterns recorded for the graphite samples. The maximum intensities for the less ordered materials appear close to the 2θ angles for graphite, what helps to estimate the average structural components size and the average distance between the crystallographic planes. On the figure 1 the diffraction patterns of four samples were shown. The intensity were displayed on logarithmic scale, which is better for such a weak reflections. The diffraction patterns of the anthracite (A) and petroleum coke (KN) are similar, the same as these for the natural (GN) and the synthetic (GS) graphite. However, the significant differences are visible between these two groups. On the anthracite diffraction pattern the only three wide reflections are visible, and they can be identified as one reflection (002), connected to three-dimensional microstructure and two reflections (10) and (11) connected to two-dimensional crystalline structure. The reflection (10) is situated nearly the model position of (100) and (110) lines for graphite, however, visible part of the (11) reflection appears close to (110) and (112) lines. The other reflections of (hkl) type typical for the crystalline structure do not appear at all. Such a diffraction pattern type is characteristic for the turbostratic structure [8,10]. On the synthetic graphite diffraction pattern at least five distinctive reflections can be pointed out: (002), (100), (101), (004) and (110).

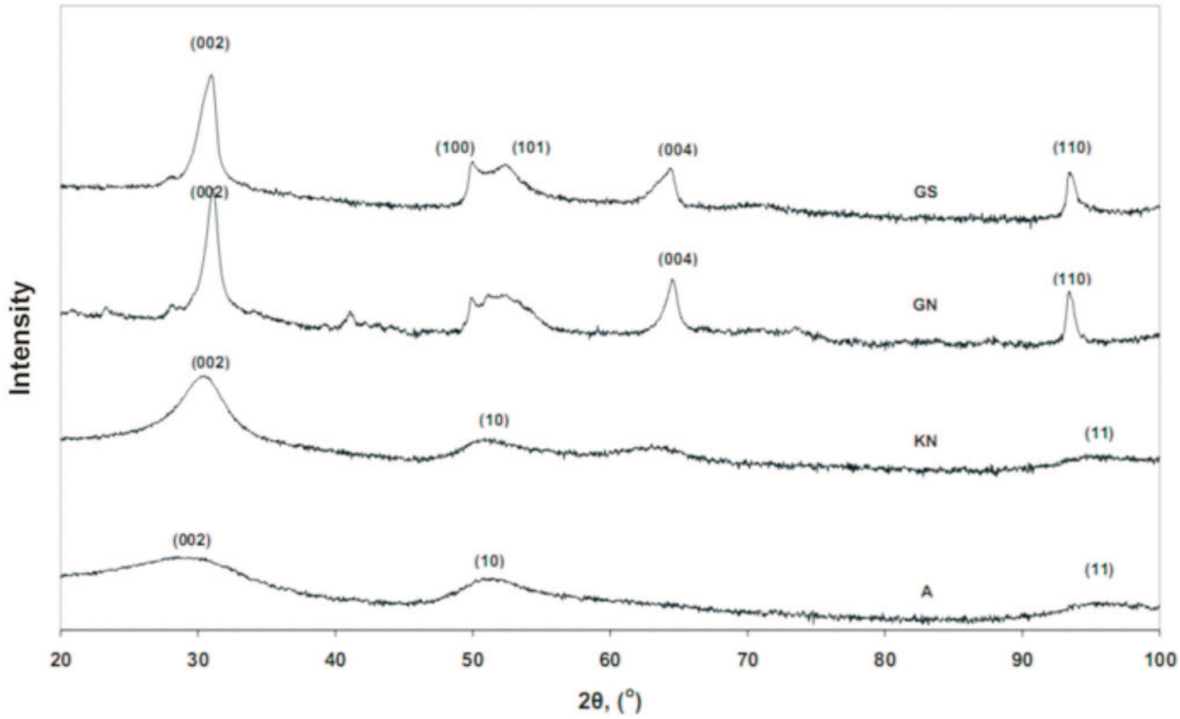

Fig. 1. The diffraction pattern for the natural graphite (GN), synthetic graphite (GS), petroleum coke (KN) and anthracite (A). The intensity is displayed on logarithmic scale

The X-ray analysis shows that the analyzed samples vary as regards crystalline degree of order. Natural and synthetic graphite are polycrystalline graphite materials. The average height of structural components (crystallite) is about 20nm and they contain app. 50-70 graphen layers, while their average diameter is about 50nm. The anthracite and petroleum coke are less ordered carbonaceous materials. The structural components (the areas where graphen layers are positioned app. parallel with the same distance between them) are definitely smaller and equal few nanometers. Also, the average distance between graphen layers is larger than recorded in graphite samples.

The samples surface morphology were analyzed on high-resolution scanning electron microscope ZEISS SUPRA 35, equipped with the chemical composition analysis system EDS [6]. On Fig. 2 the anthracite morphology (A) was presented. Similarly as for the natural graphite (Fig.3), for small magnification, the surface looks smooth and compact. In many places the mineral inclusions appear, which contain generally Mg, Ca, Fe, S and Al and C and O. With higher magnifications (20kx) the pores appear – some of them are of spherical shape. The flakes or the leaves of the graphite were not observed, however, it is visible that the sample is not compact and the pores and crevices are parallel in many places. On Fig. 3 the natural graphite (GN) morphology was presented. Even for small magnifications 4kx the surface is smooth and compact, however, on the photographs taken with greater magnifications the flat graphite flakes appear. On Fig. 4 the synthetic graphite (GS) morphology was presented. Irregular surface shape is visible even for 2kx. Empty areas (pores) of various shapes and size occur between curved layers. For greater magnifications it could be observed that cracks and crevices are parallel, while the whole sample consists of much defected layers – graphite leaves, in which densely appear small mineral inclusions. Distinct from graphite flakes, which are flat (Fig. 3), the graphite leaves may be strongly curved. Their edges are irregular and fuzzy. On Fig. 5 the petroleum coke morphology (KN) was presented. The chosen surface areas vary one from another much. Some of them are built of layers of parallel situated folds and graphite leaves. In some parts of analyzed sample, especially during the low magnification observation, the surface is smooth but cracked. On higher magnifications they are visible coiled significantly fuzzy graphite leaves which create coils. In their middle and between them the empty spaces remain – the pores. On Fig. 6 the cupola coke morphology was presented (KO). On high magnifications the graphite flakes may be observed similarly as for natural graphite. For the charcoal (Fig. 7) the regular round pores are visible on high magnifications.

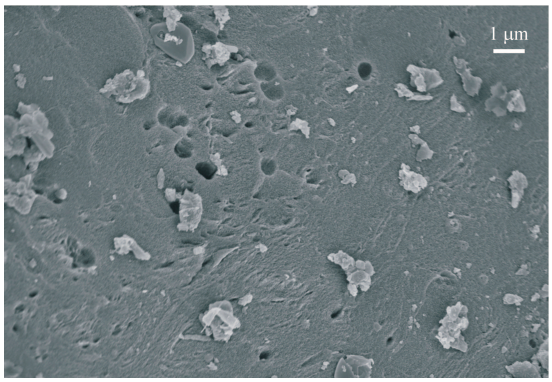

Fig. 2. The morphology of the anthracite surface (A)

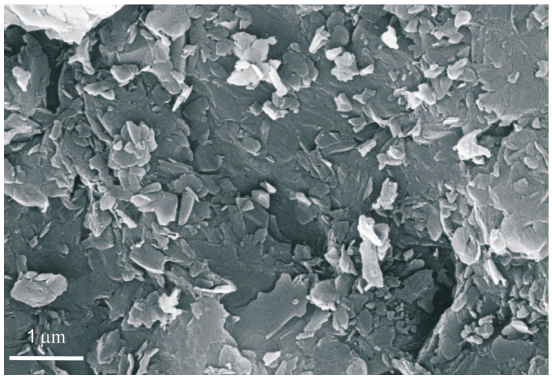

Fig. 3. The morphology of the natural graphite (GN)

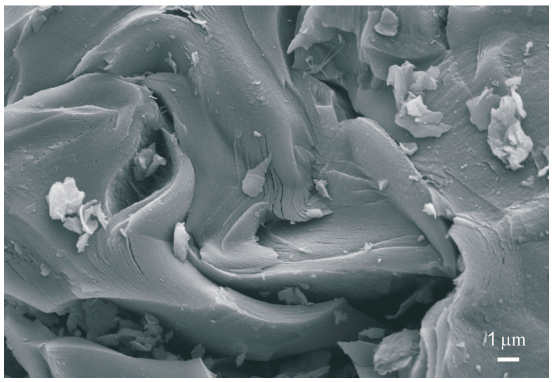

Fig. 4. The morphology of the synthetic graphite (GS)

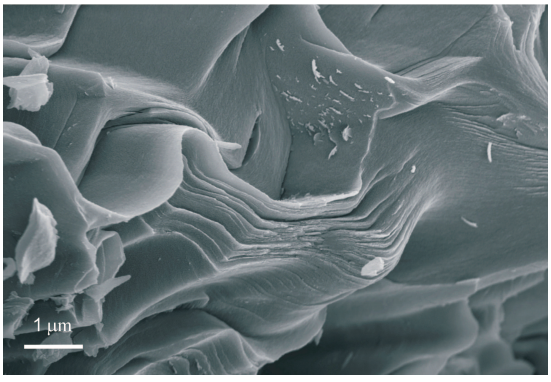

Fig. 5. The morphology of the petroleum coke (KN)

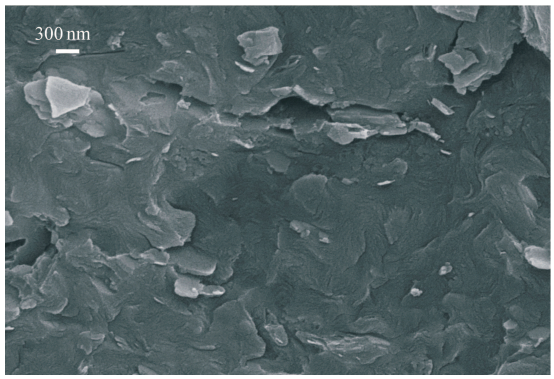

Fig. 6. The morphology of the cupola coke (KO)

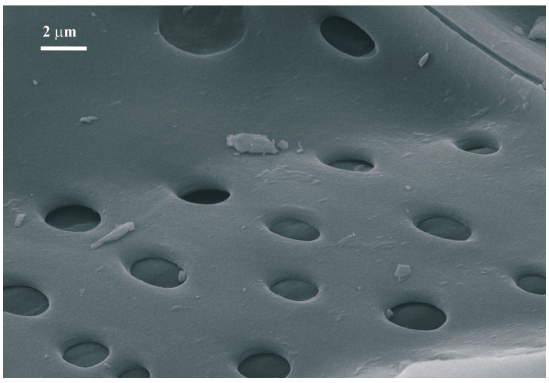

Fig. 7. The morphology of the charcoal (WD)

3. Properties and microstructure of the cast iron

During the experiments the melts of grey cast iron exclusively on the steel scrap and various carburizers basis and on the pig iron basis (S) were carried out. The melts were done in a high frequency induction furnace of 20kg capacity. The chemical composition of obtained cast iron and the average strength and hardness values were presented in Table 2.

TABLE 2
The chemical composition, tensile strength and hardness of the cast iron during the experiments

Type of carburizer	C %	Si %	Mn %	P %	S %	UTS MPa	BHN
Natural graphite GN	3.21	2.16	0.38	0.026	0.028	277	207
Synthetic graphite GS	3.30	1.96	0.46	0.033	0.024	294	221
Anthracite A	3.20	1.80	0.40	0.030	0.020	260	193
Petroleum coke KN	3.34	1.96	0.48	0.043	0.047	273	210
Cupola coke KO	3.00	2.15	0.56	0.052	0.033	350	241
Charcoal WD	3.17	1.95	0.57	0.025	0.015	262	194
Pig iron S	3.32	1.95	0.57	0.044	0.020	271	197

When compare the average tensile strength and hardness (obtained for recarburization with use of several carburizers of the same type) of the synthetic cast iron and that produced on the pig iron basis under laboratory and industrial conditions it may be observed that the results are very similar [2]. It suggests that the cast iron produced on the steel scrap basis in not worse than that melted on the pig iron basis. After the carburizer influence on the mechanical properties analysis it is difficult to point out the undoubtedly best carburizer. On that stage of experiments the conclusion that carburizer type does not significantly influence the strength and hardness of the cast iron may be drawn.

3.1. X-ray microstructure analysis

The X-ray analysis of the samples were carried out on X-ray apparatus Panalytical X´Pert PRO with use of belt detector in the angles range 2θ 25-130° (λ_{Co}= 1.78901, step 0.05, time of impulses counting 10s). The X-ray qualitative phase analysis shown that there is Fe and the cementite in analyzed materials what is proved by reflections from crystallographic planes of these phases. The diffraction patterns of the synthetic cast iron recarburized with various carburizers and the iron melted on the pig iron basis (S) were presented on Fig. 8.

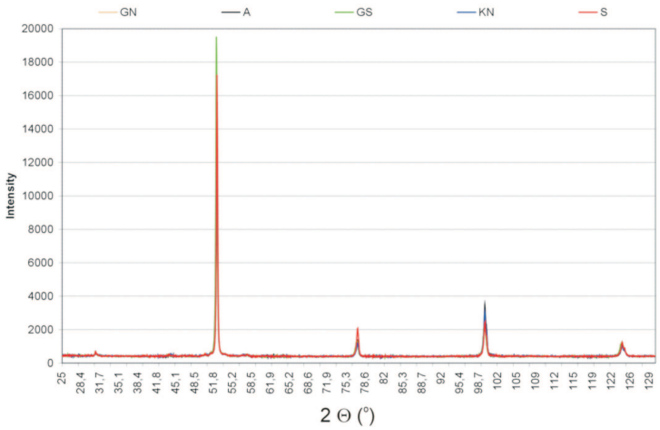

Fig. 8. The synthetic and on the pig iron basis (S) cast irons diffraction patterns

After carried out analysis it can be stated that for all alloys the same reflection for the same angles were recorded. The researches do not show any differences among the microstructures of the synthetic cast iron with various carburizers and that melted on the pig iron basis.

3.2. Derivative Thermal Analysis

There are many methods for examination of the finished castings but for the liquid alloy the most popular is Derivative Thermal Analysis (DTA) method [18,19]. Several DTA curves recorded during the experiments were presented on Figs. 9-14.

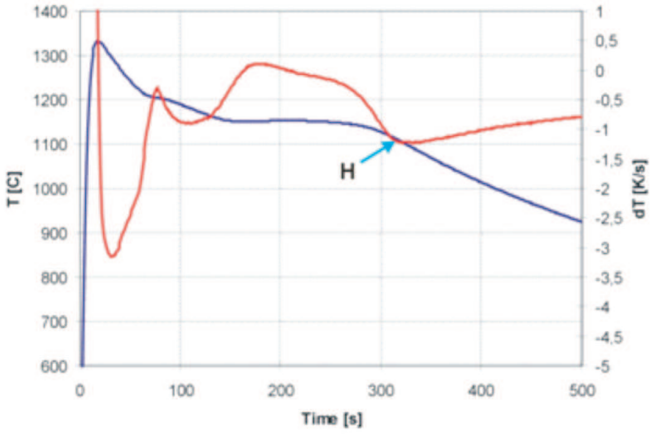

Fig. 9. DTA curves for the cast iron melted on pig iron basis (S)

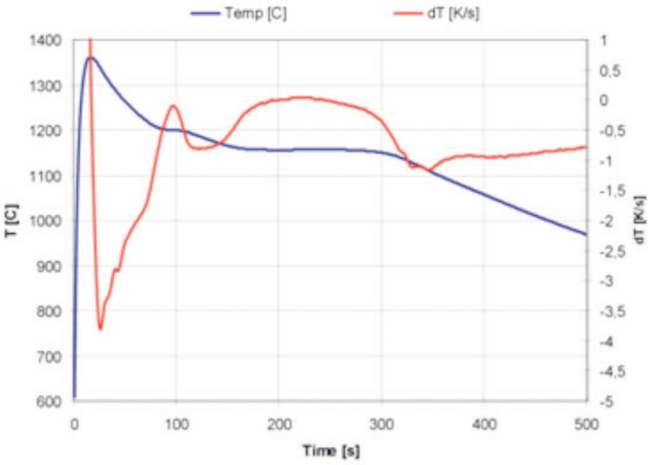

Fig. 10. DTA curves for the cast iron recarburized with the synthetic graphite (GS)

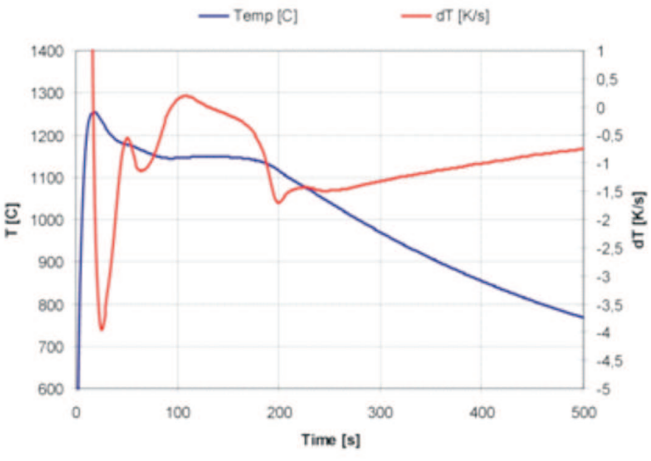

Fig. 11. DTA curves for the cast iron recarburized with anthracite (A)

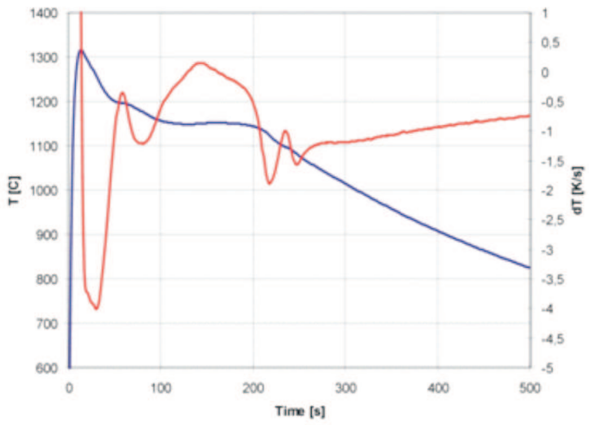

Fig. 12. DTA curves for the cast iron recarburized with petroleum coke (KN)

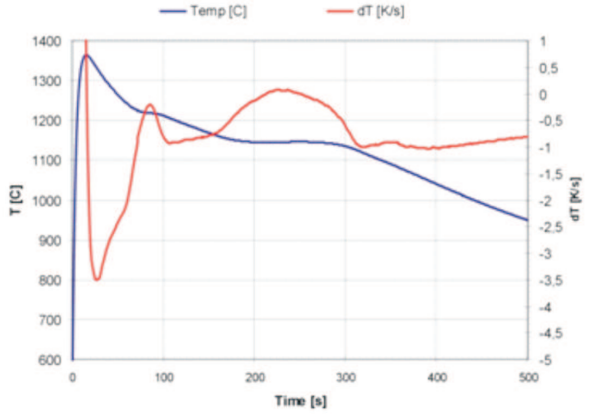

Fig. 13. DTA curves for the cast iron recarburized with cupola coke (KO)

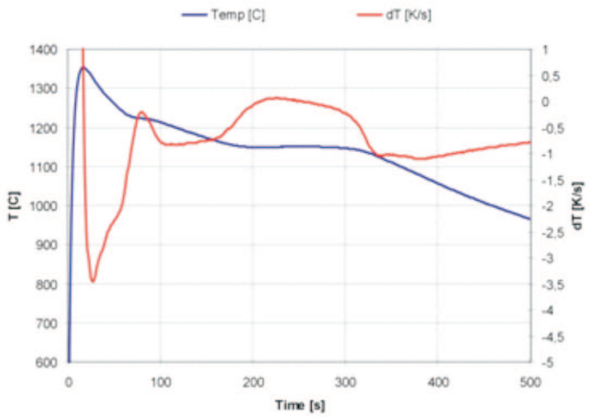

Fig. 14. DTA curves for the cast iron recarburized with charcoal (WD)

During the cooling and crystallization curves analysis obtained by DTA it can be observed that some thermal effect on the derivative curve occurs in the temperature range 1030-1130 Celsius degrees for the cast iron recarburized with petroleum coke (KN). It is not visible on the DTA curves of iron melted on the pig iron basis. H point on the crystallization curve is interpreted as the end point of the primary crystallization (solidification) what means that the last drop of the liquid metal comes into solid inside sampler in that point. The beginning of the nucleation and crystallization for all melts occurs in similar temperature range. The end of iron crystallization was at temperature close to 1100 Celsius degrees for pig iron while at app. 1130 Celsius degrees for the petroleum coke (KN). For the pig iron and the synthetic cast iron recarburized with synthetic graphite, cupola coke and charcoal the primary crystallization end point was after app. 320s and for the synthetic iron recarburized with the anthracite and petroleum coke was significantly shorter and equal 220-250s.

3.3. Microstructures of produced cast iron

The metallographic samples of the cast iron melted on the pig iron basis and synthetic cast iron were prepared during the experiments. Next, on the metallographic and scanning microscope the photomicrographs of the analyzed structures were taken. Ten photos were taken for each sample at 100x magnification. The quantitative analysis were carried out with use of Nikon NIS Elements BR 3.0 image analysis software. The structure examples were shown on Figs. 15-18 and some of the quantitative analysis results were presented in Tab. 3.

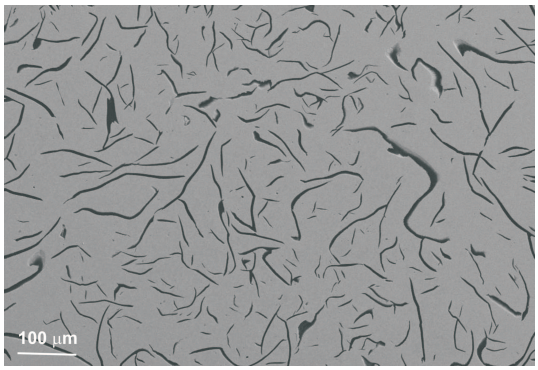

Fig. 15. The microstructure of cast iron melted on the pig iron basis (S)

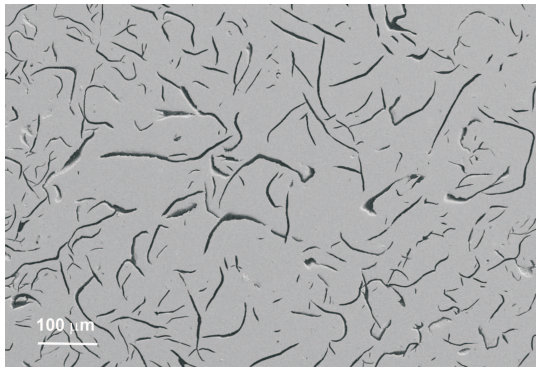

Fig. 16. The microstructure of cast iron recarburized with natural graphite GN

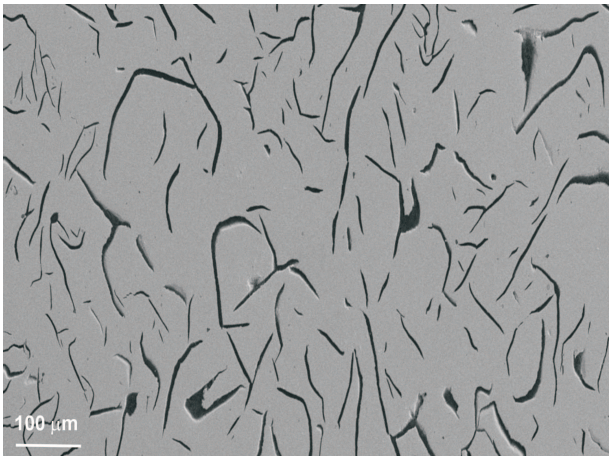

Fig. 17. The microstructure of cast iron recarburized with the petroleum coke (KN)

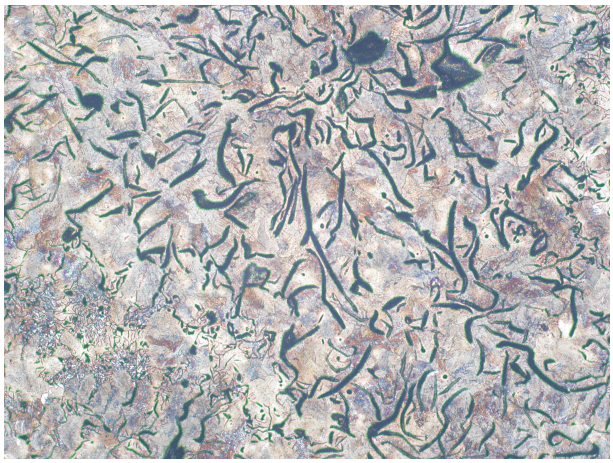

Fig. 18. Microstructure of cast iron melted on pig iron basis (S), etched in Nital (100x)

TABLE 3

The average, minimum and maximum values of the graphite precipitates parameters

Iron recarburized with:		Surface [µm^2]	Length [µm]	Width [µm]	Circularity* [µm]	Precipitates number
Synthetic graphite GS	min.	0.47	0.68	0.68	0.026	4830
	max.	6655.2	894.6	27.1	1	
	average	229.4	33.1	3.55	0.662	
Petroleum coke KN	min.	0.47	0.68	0.68	0.026	6311
	max.	7444.3	943.8	20.1	1	
	average	158.1	29.4	3.06	0.668	
Anthracite A	min.	0.47	0.68	0.68	0.011	4350
	max.	7855.5	908.3	28.9	1	
	average	262.6	39.6	3.93	0.584	
Charcoal WD	min.	0.47	0.68	0.68	0.030	3112
	max.	7893.4	903.0	21.1	1	
	average	265.4	35.4	3.30	0.638	
Cupola coke KO	min.	0.47	0.68	0.68	0.044	5186
	max.	6920.0	762.2	26.1	1	
	average	202.5	29.2	3.83	0.638	
Iron on the pig iron basis (S)	min.	0.47	0.68	0.68	0.026	6926
	max.	5243.0	799.0	19.6	1	
	average	160.6	29.9	3.38	0.676	

* Circularity is equal 1 only for circles; other shapes have this parameter less than 1. It is calculated on the object area and circumference basis. This feature is especially useful for the shapes characteristics analysis. Circularity = $4^{*}\pi^{*}$Area/Circumference^2 [20].

After analysis of the results given in Table 3 it was observed that the average parameters for cast iron melted on pig iron basis and recarburized with petroleum coke are very similar. It is true both for graphite precipitations and surface, length and circularity. The most from these materials differ from the results obtained for cast iron recarburized with charcoal and anthracite, where the precipitation number is significantly lower but their size is bigger. It is for sure an effect that there are considerably less areas with small interdendritic graphite on the cast iron recarburized with charcoal metallographic samples. Very similar parameters have graphite precipitates in cast iron recarburized with cupola coke and synthetic graphite. The described analysis was carried out on samples taken from one melt for each carbu-

rizer. Besides the analyzed objects number is high, the conclusions about the carburizer grade influence on the cast iron microstructure will be worked out after calculations made for other melts with the same carburizers. Because of the limited space in the paper the histograms of the particular values were not included.

The quantitative analysis of the graphite precipitations were completed with qualitative analysis of analyzed cast iron microstructure. The examples of the iron structures obtained on the pig iron basis and steel scrap basis with various carburizers were presented on figures 18-20. The cast iron matrix is almost identical for all cases and consist mostly of pearlite with only ferrite traces. Greater differences are for the graphite precipitates, the iron structures vary much in shape and flakes size of graphite. Particularly for the cast iron melted on the pig iron basis apart from typical graphite precipitation present in this cast iron grade normally the tiny interdendritic graphite precipitations are visible, too.

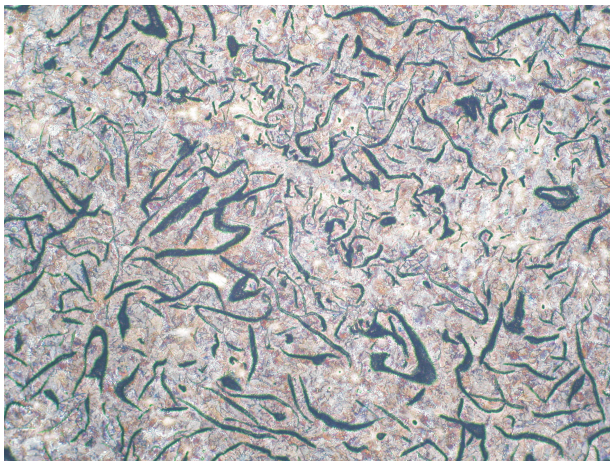

Fig. 19. Microstructure of cast iron recarburized with natural graphite (GN), etched in Nital (100x)

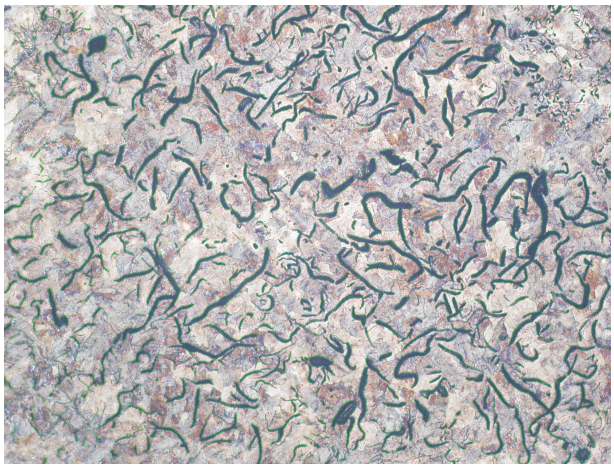

Fig. 20. Microstructure of cast iron recarburized with petroleum coke (KN), etched in Nital (100x)

4. Summary

After the all carried out experiments it may be stated that carburizers vary not only in chemical composition but the microstructure degree of order and its morphology, too.

When cast iron melted on the pig iron basis and these recarburized with various carburizers were compared it was concluded that there are only small differences in tensile strength and hardness between all of them. After chemical composition analysis it may be stated that synthetic cast iron contains generally less impurities level because there is less sulfur and phosphorus content in steel scrap. The differences in results of qualitative phase analysis was not present as well and peaks from particular angles are almost identical, too.

Some differences can be observed for solidification and crystallization curves. This is particularly distinct at primary crystallization end point (H point). For the cast iron melted on the pig iron basis the curve shape in this area is rather ”gentle” and for the synthetic cast iron there are additional thermal effects with intensity depends on the carburizer grade.

The differences are for the cast iron microstructures, too. This is particularly visible during quantitative analysis of the precipitates but on present researches stage it is impossible to undoubtedly say that the cast iron structure is directly dependable on used carburizers grades.

Acknowledgements

This research project was financed from support funds for science during 2009-2011.

REFERENCES

[1] K. Janerka, D. Bartocha, J. Szajnar, M. Cholewa, The influence of different kind of carburizers and recarburization on the effectiveness and iron structure, Archives of Metallurgy and Materials **52**, 3, 467-474 (2007).

[2] K. Janerka, D. Bartocha, J. Szajnar, Quality of carburizers and its influence of recarburization process, Archives of Foundry Engineering **9**, 3, 249-254 (2009).

[3] K. Janerka, D. Bartocha, The sort of recarburization and the quality of obtained cast iron, Archives of Foundry Engineering **8**, 4, 55-60 (2008).

[4] K. Janerka, The rate of effectiveness of recarburization to the sort of carburizer, Archives of Foundry Engineering **7**, 4, 95-100 (2007).

[5] K. Janerka, J. Jezierski, M. Pawlyta, The properties and structure of the carburiz-

ers, Archives of Foundry Engineering **10**, 1, 67-74 (2010).
[6] L.A. Dobrzanski, M. Pawlyta, W. Kwasny, K. Janerka, The structure of the carbonaceous materials used for cast iron recarburization, Karbo, Wydawnictwo Gornicze, Zabrze, 2, 91-98 (2009) (in Polish).
[7] K. Janerka, The recarburization of the liquid ferrous alloys, Wydawnictwo Politechniki Slaskiej, (2010), (in Polish).
[8] D. Bartocha, K. Janerka, J. Suchon, The influence of charging materials and melting technology on the ductile cast iron properties, Archiwum Odlewnictwa **5**, 17, 17-26 (2005) (in Polish).
[9] D. Bartocha, J. Gawronski, K. Janerka, The relationship between cast iron properties and charging materials **3**, 9, , 22-30 (2003) (in Polish).
[10] K. Janerka, D. Bartocha, Computer simulation of carburizers particles heating in liquid metal, Archives of Foundry Engineering **10**, 1, 59-66 (2010).
[11] D. Bartocha, K. Janerka, Carburizer particle dissolution in liquid cast iron, Archives of Foundry Engineering **10**, 1, 7-14 (2010).
[12] J. Tybulczuk, K. Martynowicz-Lis, M. Pachota, A. Kryczek, Polish foundry industry in 2007, Foundry Research Institute, Krakow 2007.
[13] K. Skoczkowski, The carbon-graphite liners, W. Swietoslawski's Foundation for Polish Science, Gliwice 1998 (in Polish).
[14] A. Kuznicka, W. Kuznicki, A. Gorny, The modern ELKEM Elgraph series carburizers, Foundry Review, 7-8 (2000) (in Polish).
[15] Biscoe and Warren, An X-Ray Study of Carbon Black, Journal of Applied Physics **13**, 364-371 (1942).
[16] B.E. Warren, X-ray diffraction in random layer lattices. Journal of Applied Physics **20**, (1996).
[17] L. Lu, V. Sahajwalla, C. Kong, D. Harris, Quantitative X-ray diffraction analysis and its application to various coals, Carbon 39(12), 1821-33 (2001).
[18] S. Jura, Alloys crystallization, differential thermal analysis (DTA), Archiwum Odlewnictwa, Special Issue, No. 16, 2004.
[19] S. Pietrowski, G. Gumienny, Methodology of ductile cast iron quality evaluation with use DTA method, Archiwum Odlewnictwa, No 6, 2002.
[20] Nikon NIS Elements, User's Manual version 3.0.

Received: 10 July 2010.